LAWRENCE
LIVERMORE
NATIONAL
LABORATORY

UCRL-PROC-211890

Improved Detection, Surveillance, and Threat Characterization via Host-Pathogen Interaction Studies

B. Chromy, C. Zhang, A. Clatworthy, I. Fodor, M. Alegria-Hartman, A. Holtz-Morris, K. Montgomery, M. Choi, T. Corzett, M. Derksen, V. Kopf, R. Mahnke, B. Ricks, K. Robbins, R. Birmingham, B. Chang, C. Corzett, A. Robbins, J. Seoane, N. Chongsiriwatana, B. Fisher, D. Schroeder, N. Drazenovich, K. Smith, J. E. Foley, S. L. McCutchen-Maloney

May 2, 2005

DHS 1st Annual National Homeland Security R&D Conference
"Research and Development Partnerships in Homeland Security"
Boston, MA, United States
April 26, 2005 through April 28, 2005

DHS 1st Annual National Homeland Security R&D Conference "Research and Development Partnerships in Homeland Security", Boston, MD, April 26-28 2005

"Improved Detection, Surveillance, and Threat Characterization via Host-Pathogen Interaction Studies"

Brett Chromy[1], Celia Zhang[1], Anne Clatworthy[1], Imola Fodor[1], Michelle Alegria-Hartman[1], Ann Holtz-Morris[1], Kris Montgomery[1], Megan Choi[1], Todd Corzett[1], Michael Derksen[1], Vicki Kopf[1], Ryan Mahnke[1], Brent Ricks[1], Kristin Robbins[1], Rachelle Birmingham[1], Brian Chang[1], Chris Corzett[1], Alexandria Robbins[1], Josefina Seoane[1], Nate Chongsiriwatana[2], Bridget Fisher[3], David Schroeder[4], Niki Drazenovich[5], Kimothy Smith[1], Janet E. Foley[5], Sandra L. McCutchen-Maloney[1]*

[1]Lawrence Livermore National Laboratory, Livermore, California
[2]Northwestern University, Evanston, Illinois
[3]University of Wisconsin, La Crosse, Wisconsin
[4]Purdue University, West Lafayette, Indiana
[5]University of California, Davis, California

* To whom correspondence should be addressed:

Ph: 925 423-5065, Em: smaloney@llnl.gov

Keywords: *Bacillus*, biodefense, host-pathogen interactions, pathogenicity, presymptomatic detection, proteomics, virulence, *Yersinia*

Abstract

In the age of bioterrorism awareness, there is an unprecedented urgency for in-depth characterization of host-pathogen interactions and establishment of a "Host Response Library" and a "Pathogen Reference Library" to curate the vast amounts of information generated from such studies. These libraries, or databases of information, could prove invaluable for detection of known, engineered, or emergent pathogens; surveillance of infectious diseases in the civilian and military populations; and subsequent threat assessment in the event of a pathogen release. Moreover, this information would server a dual use in the event of a outbreak, be it intentional, accidental or natural, to screen the large number of individuals that may have been exposed and for rapid risk assessment. *Yersinia pestis* and *Bacillus anthracis*, the etiological agents of plague and anthrax, mark two threats of considerable concern to human health from a civilian biodefense perspective. Characterization of host-pathogen interactions using diverse host models and diverse pathogens has afforded a means to identify next-generation signatures that are pathogen specific and that can identify a pathogen exposure based on host response. Toward this end, we have identified host signatures that can distinguish *B. anthracis* from *Y. pestis* exposure; *Y. pestis* from near neighbor exposures; and avirulent from virulent pathogen exposures. Most notably, two *Y. pestis* clinical isolates, determined to exhibit 1000-fold difference in virulence as determined in rodent challenges, can be distinguished from each other based solely on host response. These results suggest that host response signatures could be used, in the absence of other information, to detect early exposure to a pathogen and to specify the pathogen in question. Further, it is technically possible to assess the threat of a pathogen based on host response combined with pathogen characteristics. In our pathogen characterization studies, categorization of diverse clinical isolates of *Y. pestis* has revealed distinct differences in proteomic content of multiple *Y. pestis* strains, with implication in virulence and lethality levels.

Introduction

Post 9/11, a shift in the direction of biodefense research has emerged with an urgency for basic, discovery-driven science to provide novel solutions for biodefense preparedness. Thus basic science has a clear role in supporting critical translational applications for Homeland Security. For example, host-pathogen interactions, which reflect the balance of host defenses and pathogen virulence mechanisms, contain key signatures or biomarkers that can be useful for presymptomatic, presyndromic and/or syndromic surveillance and for unveiling virulence characteristics of a pathogen. Here, we focus on host-pathogen interactions of *Yersinia pestis* and *Bacillus anthracis*, the etiological agents of plague and anthrax. Notably, many early symptoms of these diseases, and other diseases of concern to national security, are flu-like and nondescript. A such, characterization of host-pathogen interactions, in particular discovery of biosignatures that can distinguish pathogen exposures and reveal virulence characteristics, promise great advances in early detection, surveillance, and clinical diagnostics with the ability to guide rapid response.

Naturally occurring plague can be transmitted from infected fleas and rodents to humans, and is a highly communicable as evidenced by three historic pandemics (REF). *Y. pestis* functions via the Type III secretion mechanism whereby virulence factors are injected into the host, and three forms of the disease exist: bubonic, septicemic and the highly contagious pneumonic form. While bubonic and septicemic forms may be less severe and readily treated with antibiotics, pneumonic plague is often fatal. In the recent plague outbreak in the Republic of Congo, 57 of 130 patients had died as of March 30, 2005 (REF), and most notable in this outbreak was the unusually high incidence of pneumonic plague. There is also an increased awareness of the threat of anthrax (REF). Three forms of the disease have been described: cutaneous, intestinal and inhalation, and while cutaneous and intestinal forms are less severe, inhalation anthrax is often fatal without prompt antibiotic treatment. The primary mechanism of virulence employed by *B. anthracis* is associated with two virulence plasmids that code for toxins [31]. To address the need for early and specific detection of plague and anthrax, we present proteomic and phenotypic categorization of diverse strains of *Y. pestis*; discuss a novel means to characterize virulence; and report proteomic, genomic, clinical, and immunohistopathological categorization of host response in rodent, cell, and whole blood models of plague and anthrax.

Methods and Materials

Pathogen Proteomic Characterization. *Yersinia pestis* bacterial cell colonies were picked from glycerol stocks and grown on tryptose blood agar plates at 26°C for 2 days. Individual colonies were selected and bacteria grown on a tryptose blood agar slant at 26°C for 2 days. The bacteria were washed off of the slants using 2 ml of 0.033 M K-phosphate, pH 7.0. Cells (1.3 ml) were lightly vortexed and diluted 100-fold into K-phosphate buffer. Next, 0.1 ml of the cell suspension was used to inoculate 15 ml of best case scenario (BCS) media in a 125 ml flask. Cells were grown at 26°C at 200 rpm for 8h and an OD_{620} between 0.6 and 0.7 (1 OD_{620} = 1.2 x 10^9 CFU/ml). 4 ml of this culture was then used to inoculate 50 ml BCS media in a 250 ml flask, which was grown at 26°C for an additional 16 h to an OD_{620} between 2.3 and 2.5. Finally, 52 ml of the second culture was used to inoculate 2.175 liters of BCS media, which was divided into eight 125 ml cultures grown in 1 liter flasks at 26°C. After 8 h of growth, four of the flasks were shifted to 37°C, two of which were supplemented with 1.25 ml of 0.4 M $CaCl_2$ solution, while the other two were supplemented with water. Similar additions of $CaCl_2$ or water were repeated for the four flasks growing at 26°C. Cells were grown for an additional 4 h after the temperature and calcium concentration shifts, providing the four different growths for proteomic analysis.

Cultures were harvested at defined phases by centrifugation and resuspended in 50 mM ammonium bicarbonate pH 7.8. Cells were washed two times in the same buffer and pelleted by centrifugation at 4,000 rpm for 10 minutes. Cell lysis was achieved by bead beating using three 180 sec cycles at 4500 rpm in a Mini-BeadBeater-1 (BioSpec Products, Inc., Bartlesville, OK), with a 5 minute cool down period on ice between cycles. Lysates were immediately placed on ice to inhibit proteolysis and 1X protease inhibitor cocktail (Roche) was added. Protein was quantified using the ADV01 reagent (Cytoskeleton) and analyzed at wavelength of 590. Following protein assay, protein extraction was performed as described in the Ettan 2-D DIGE users guide (Amersham). Briefly, oligonucleotides and other non-protein contaminants were removed by using the 2-D protein cleanup kit (Amersham).

2-D DIGE Analysis. Samples from each of the four growth conditions were aliquoted (50 μg) and labeled with the fluorescent amine-reactive cyanine dyes, Cy3 or Cy5 CyDyes (200 pmol, see Table 1). For the internal pooled standard, equal amounts of all four samples were pooled and 50 μg aliquots were labeled with 200 pmol of Cy2. This pooled standard was used in each gel to normalize protein abundance measurements across each gel facilitating inter-gel spot matching and relative protein quantitation. After labeling protein of each experimental growth sample and the pooled standard with CyDyes for 30 minutes at 4°C, the labeling reaction was quenched with 1 nmol of lysine. Eight gels were used for each experiment and multiplexed analysis was performed according to Table 1. In addition to the fluorescently labeled samples, in two of the gels, additional unlabeled protein sample (50 μg) from each growth condition was added to ensure enough protein was present for subsequent protein identification by mass spectrometry. Multiplexed samples were separated by charge on 24 cm 3-10 NL Immobiline IPG DryStrips, and separated by size on 12.5% polyacrylamide gels. Following electrophoresis, gels were scanned using the Typhoon 9410 imager and protein spots were analyzed using DeCyder™ software.

Table 1. Experimental design for 2-D DIGE experiment.

Gel Number	Cy3 Labeled Sample	Cy5 Labeled Sample	Cy2 Labeled Sample	Additional Unlabeled Sample
Gel 1	50 μg 26°	50 μg 37v	50 μg pooled standard	
Gel 2	50 μg 37° w/ Ca	50 μg 26°	50 μg pooled standard	
Gel 3	50 μg 26°	50 μg 26° w/ Ca	50 μg pooled standard	
Gel 4	50 μg 26° w/ Ca	50 μg 37°	50 μg pooled standard	
Gel 5	50 μg 26° w/ Ca	50 μg 37° w/ Ca	50 vg pooled standard	
Gel 6	50 μg 37°	50 μg 37° w/ Ca	50 μg pooled standard	
Gel 7	50 μg 26° w/ Ca	50 μg 37°	50 μg pooled standard	50 μg each growth
Gel 8	50 μg 37° w/ Ca	50 μg 26°	50 μg pooled standard	50 μg each growth

2-D DIGE gel images were subjected to DeCyder analysis. CyDye images from individual gels were analyzed by differential in gel analysis, (DIA) and protein spots were detected. Differential protein expression was determined between two samples in the gel based on the ratio of standardized log of abundance of the Cy3 versus Cy5 spot volume over the Cy2 spot volume. The standardized log of abundance is the log abundance of the Cy3- or Cy5-labeled spot over the log abundance of Cy2-labeled pooled standard spot. T-test values were obtained by comparing the differential expression of the Cy3/Cy2 volume as compared to Cy5/Cy2 volume. CyDye images from all the gels within the experiment were then analyzed by biological variation analysis, (BVA). Protein spots were normalized to the Cy2 spot volumes. T-test values were obtained by comparing all the replicates from one sample compared to another. Differential spots reported in the text have p values less than or equal to 0.05. DeCyder analysis provided a pick list file containing the pixel location of the differentially expressed protein spots of interest. Protein spots were picked using the ProPic Robotic Workstation (Genomic Solutions) using a custom software and hardware to integrate DeCyder Analysis with the ProPic Workstation (R.C. Mahnke and B.A. Chromy, in preparation). Each experiment contained three gel replicates of each of the four growth conditions, and the entire experiment was performed four times.

Protein spot digestion and mass spectrometry characterization were performed by Proteomic Research Services (PRS, Ann Arbor, MI). Differentially expressed protein spots were subjected to robotic in-gel digestion using trypsin (ProGest) following reduction with DTT and alkylation with iodoacetamide. A portion of the resulting digest supernatant was used for matrix assisted laser ionization desorption-mass spectrometry (MALDI-MS) analysis. Spotting was performed robotically (ProMS) with ZipTips; peptides were eluted from the C18 material with matrix (α-cyano 4-hydroxy cinnamic acid) in 60% acetonitrile, 0.2% TFA. MALDI-MS data was acquired on an Applied Biosystems Voyager DE-STR instrument and the observed m/z values were submitted to ProFound for peptide mass fingerprint searching using the NCBInr database. Those samples that proved inconclusive following MALDI-MS were analyzed by LC/MS/MS on a Micromass Q-TOF2 mass spectrometer using a 75 μm C18 column at a flow-rate of 200 nl/min. The MS/MS data were analyzed using MASCOT.

Phenotype Arrays. Phenotype microarray plates were inoculated with *Y. pestis,* incubated under one of the 4 growth conditions, and the dye intensities were measured in an Omnilog® robot (Biolog, Hayward, CA) every 15 minutes for 3 days. The controlling software then converts the digital images to dye intensity values[i].
Per the manufacturer's instructions, homogenous cell suspensions were diluted to 85%T in a turbidimeter in 1X GN IF-0 medium(Biolog). All plates are supplemented with 1mM Sodium thiosulfate. Plates PM1 and PM2A were inoculated with this minimal medium. 20mM Potassium gluconate, pH 7.0 the carbon source was added to plates PM 3B, 4A, 5, 6, 7 and 8. Calcium chloride, if added, was added to 4mM final concentration. Because calcium speeds the gelling reaction, it was necessary to add it immediately prior to inoculation. Dye values (minus negative control) for 3 replicates of each condition are plotted over time. Spontaneous mutants were not removed from data. Because preliminary tests indicated that Dye mix A and Dye mix B caused toxicity to the Y. pestis KIM D27 cells under the 37°C without Calcium growth condition, Dye mix D was utilitzed throughout the inoculum. The PM technology for microbial cells contains 20 micro plates. Eight micro plates contain compounds related to the main catabolic pathways for carbon, nitrogen, phosphorous and sulphur, as well as biosynthetic pathways. One plate tests osmotic stress factors and ion effects. Another one investigates pH growth range and pH regulation. Ten plates test the sensitivity of cells to a number of chemicals, such as antibiotics, anti-metabolites, membrane-active agents, respiratory inhibitors, and toxic metals. An additional 10-plate set of antibiotics is also included.

Real-Time Virulence Reporter. The GFP plasmid pEGFP was obtained from Clontech (Mountain View, CA). All media used for the culture of clones bearing derivatives of pEGFP vector were supplemented with carbenicillin to 50 μg/mL. All reporters were created as described in (Cam's BBRC). Briefly, reporter strain cultures are grown in WCS media (minimal media supplemented with carbenicillin (50 μg/mL) and with or without 4 mM $CaCl_2$ until saturation. Bacteria are then resuspended in fresh WCS media to a cell density in the range of 10^7-10^8 cfu/mL and aliquoted into a 96-well plate (200 □L/well). Wells are overlayed with mineral oil (50 μL/well) and incubated in a Victor2 plate reader (Perkin Elmer) with

shaking at 26°C for 16 hours at which point the temperature is raised to 37°C for ≥24 hours. The Victor2 plate reader obtains optical density and fluorescence measurements between repeated cycles of shaking (1mm orbital, normal speed, 30 min) over this time period.

Cell Exposures. The human monocyte cell line, U937 (CRL-1593.2) was obtained from ATCC and maintained as frozen stock at –80°C in RPMI-1640 medium containing 10% fetal bovine serum, 1% penicillin-streptomycin and 10% dimethyl sulfoxide. The U937 cells were grown in RPMI-1640 medium supplemented with 10% fetal bovine serum and 1% penicillin-streptomycin solution in a 5% CO_2 incubator at 37°C to log phase (1.2×10^6 cells/mL). Cells were then spun down at 800 g for 5 min and suspended in a fresh RPMI-1640 medium without supplements. Ten milliliters of suspension culture containing 3×10^7 cells was placed in each cell culture dish (VWR 25382-442). Cells were allowed to attach to the cell culture dish for 2 hours in a 5% CO_2 incubator at 37°C, and cells were then subjected to pathogen exposure. Exposures to *Y. pestis*, *Y. enterocolitica* and *Y. pseudotuberculosis* were performed as described in (BBRC and Proteomics). Cytoplasmic and nuclear proteins were extracted from the cell pellets described above with NE-PER Nuclear and Cytoplasmic Extraction Reagents (Pierce) as described by the manufacturer. Membrane proteins were extracted with Mem-PER Eukaryotic Membrane Protein Extraction Reagent kit (Pierce). Halt Protease Inhibitor Cocktail (Pierce) was added to protein extraction reagents prior to extraction at a final concentration of 10 µl/mL to reduce protein degradation. Protein concentrations were measured using the Advanced Protein Assay Reagent (Cytoskeleton Cat# ADV01). 2-D DIGE analysis and protein identification were performed as above.

Whole Blood Exposures.B. anthracis Ames (virulent), *B. anthracis* Sterne (attenuated), *Y. pestis* KIM D27 (avirulent), *Y. pestis* India (virulent), and *Y. pestis* NYC (virulent), *Y. pseudotuberculosis* serotype 1 PB1, and *Y. enterocolitica* WA serovar 0:8 were grown on tryptose blood agar slants at 26 °C for 2 days. The bacteria were washed off of the slants using 2 ml of 0.033M potassium-phosphate, pH 7.0 and the bacterial densities were measured at OD_{620} ($1\ OD_{620} = 1.2 \times 10^9$ colony forming units/ml). Human blood was collected from one healthy donor by venipuncture using CPT vacutainer tubes (Becton Dickinson) containing citrate as anti-clotting agent. The whole blood was divided into 8 aliquots for 8 treatments including control and 7 different bacterial exposures (*B. anthracis* Ames, *B. anthracis* Sterne, *Y. pestis* NYC, *Y. pestis* India, Y. *pestis* KIM D27, *Y. pseudotuberculosis*, and *Y. enterocolitica*). Bacteria were added to blood within 15 minutes of collection in a multiplicity of infection ratio of 5:1 (ratio was determined against estimated white blood cells in whole blood: 7×10^6 cells/ml). The whole blood was incubated with bacteria for 4 hours at 37 °C in 5% CO_2. Following incubation, plasma was collected by centrifugation of the blood at 2000 x g for 10 min at 4 °C. The uninfected control plasma was obtained in the same way except without bacterial exposure. Plasma was stored at -80 °C for future use. The eight human plasma samples were analyzed in triplicate using Zyomyx Protein Profiling Biochips (Hayward, CA). A total of 30 human cytokines can be tested simultaneously with Zyomyx human cytokine biochips. The 30 cytokines are: Eotaxin, G-CSF, GM-CSF, IFN-γ, IL-10, IL-12(p40), IL-12(p40/p70), IL-12(p70), IL-13, IL-15, IL-1α, IL-1β, IL-2, IL-3, IL-4, IL-5, IL-6, IL-7, IL-8, IP-10, MCP-1, MCP-3, MIG, sCD23, sCD95(sFas), sICAM-1, TGF-β, TNF-α, TNF-β, and TRAIL. Each of plasma samples was injected, in the volume of 40 µl, onto the chips in triplicates. Cytokine assays were performed using Zyomyx Assay 1200 Workstation according to the manufacturer's instruction. Cytokine chips were scanned with Zyomyx Scanner 100 after cytokine assays. Zyomyx Data Reduction software was used for normalization of data, calculation of calibration curves, and quantification of cytokines in samples by calibration to a known standard.

Rodent exposures. All experimental work was performed subject to oversight of institutional animal care and use committees at UC Davis and LLNL in full compliance with AAALAC requirements. Bacterial doses to induce mortality in 50% of BALB/c mice inoculated IP were determined by the "revised up and down method" for establishing an ED (effective dose) $_{50}$ (ICCVAM et al., 2001). Ultimately, the following quantities of bacteria produced high morbidity and/or death on day 4 post-infection (PI) in half of the mice and were used for subsequent inoculation: 5×10^4 of *Y. pestis* NYC, 1×10^7 of *Y. pestis* India-195, which were each inoculated IP into five 10 wk old, male BALB/c mice that had been anesthetized with 40 mg/kg ketamine and 4 mg/kg xylazine SC. Control mice were inoculated only with saline IP. Follow-up evaluation included physical examination and blood collection for cytokine assessment, complete blood count, bacterial culture and PCR on days 0 (before infection) and 3 PI, as well as complete necropsy when mice were terminally ill. On day 3, anesthetized mice were exsanguinated by cardiac puncture, euthanized while anesthetized by cervical

dislocation, and necropsied. Necropsy included gross examination of all internal organs and collection for culture, PCR, and histopathology of samples of spleen, liver, and lungs. Proteomic characterization by 2-D DIGE is in progress.

Results and Discussion

Yersinia pestis Proteomic Characterization. It is known that alteration in physiological growth conditions from the temperature and calcium concentration found in the flea vector to that found in the mammalian host can trigger virulence-related expression in *Y. pestis* [73, 74] (**Figure 1**). Proteomic analyses of *Y. pestis* grown under 26°C and 4 mM calcium (mimicking flea); 37°C and 4 mM calcium (mimicking host bloodstream); and 37°C and 0 mM calcium (mimicking host intracellular) have revealed distinct protein expression patterns between these relevant pathogen states [17-19]. Previously, multiplexed 2-D difference in gel electrophoresis (DIGE) and mass spectrometry were reported, which characterized the *in vitro* induction of the Type III secretion virulence mechanism [18]. In this study, 375 proteins were differentially expressed between the temperature and calcium growth conditions above, of which 43 were identified. Several known virulence-associated factors were identified under the growth conditions mimicking the host including catalase-peroxidase, murine toxin, plasminogen activator, and F1 capsule antigen. Other differentially expressed proteins with possible relevance to virulence include proteins involved in sugar metabolism as well as several chaperone proteins and signaling molecules hypothesized to be involved in virulence due to their role in Type III secretion. This represents a quantitative comparative proteomic approach that has been extended to compare same species strains of different virulence levels in which we have demonstrated the ability to distinguish multiple clinical isolates of *Y. pestis* based on proteomic content.

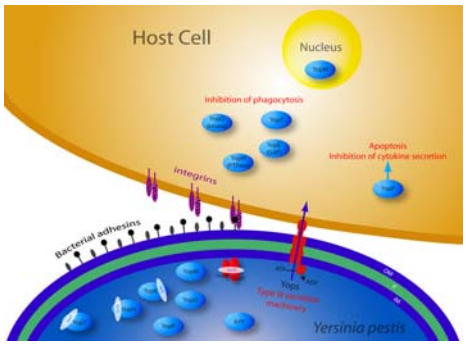

Fig 1. Host-pathogen interaction model of *Yersinia pestis*, depicting the Type III secretion mechanism.

For example, we have used 2-D DIGE to compare two isolates, *Y. pestis* NYC and India-195, which exhibit over 1000-fold differences in pathogenicity as determined in a rodent model **(Figure 2**). Results indicated that Ymt, the *Yersinia* murine toxin, is upregulated in the NYC strain, which corroborates the higher lethality level of this strain in rodents. Moreover, we also determined that PLDA, a phospholipase membrane protein, was differentially expressed in the NYC strain, with one protein spot of PLDA upregulated and another downregulated, potentially due to post-translational modification or processing to an active isoform. Notably, this protein is a known virulence factor in *Y. pseudotuberculosis*, and is implicated in anti-inflammatory response to pathogenic *E. coli*. There are however no previous reports to our knowledge with regard to virulence of the PLDA protein in *Y. pestis*. Additional differentially expressed proteins are under investigation. From a biodefense viewpoint, differentially expressed proteins identified from proteomic comparison of diverse strains have application for detection and threat assessment. Moreover, comparison of diverse strains, in particular highly virulent strains, may identify virulence determinants useful in characterization of unusual isolates, emergent, or engineered pathogens.

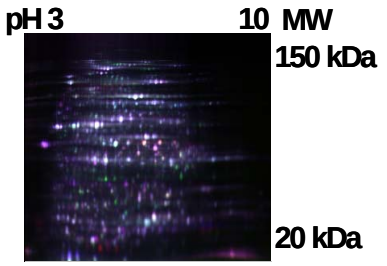

Fig. 2. Multiplexed 2-D DIGE, differentially expression between 2 *Y. pestis* clinical isolates, indicated by color.

Phenotypic Characterization. Traditional means to test bacterial phenotypes have involved growing bacteria on specialized culture media on petri plates or in liquid broth cultures followed by visual inspection. Thus realistically, this type of characterization could examine the effects of fewer than 30 chemicals at a time. A high-throughput phenotype microarray technology (Biolog Inc, Hayward, CA) now provides the ability to simultaneously test thousands of phenotypes in an automated in 96 wells preloaded with approximately 2000 nutrients. If an organism can metabolize one of the 2000 nutrients, cells grow, indicating a functional metabolic pathway. The resulting kinetic (growth curve) profiles are recorded in real time. Differences in the growth curves observed under

varying physiological growth conditions, or between diverse isolates of *Y. pestis*, indicate biological differences with possible implication in virulence. To address, phenotypic differences under virulence-inducing growth conditions, we studies *Y. pestis* under four biologically relevant conditions, and measured cell growth every fifteen minutes for three days. The calcium concentration and the temperature represented the flea midgut (26° C, 4 mM Ca), mammalian host plasma (37° C, 4 mM Ca), and host intracellular (37° C, 0 mM Ca) physiological condition, were used, and an additional control (26° C, 0 mM Ca), was also tested. **Figure 3** shows the data from a subset of the 2000 phenotypes tested.

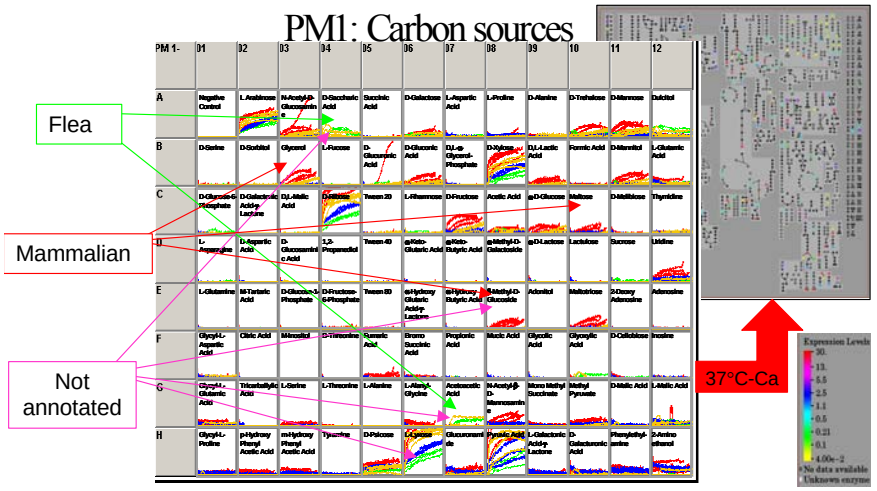

Fig 3. Growth of *Y. pestis* depends on the condition. The colors correspond to the four biologically relevant conditions mimicking: flea midgut (26° C, 4mM calcium, green), mammalian host plasma (37° C, 4mM calcium, yellow), host intracellular (37° C, 0mM calcium, red), and control (26° C, 0mM calcium, blue). Note that the map is computationally derived without curation, and pathways can be characterized based on phenotype.

Through our initial experiments, we found evidence of the existence of biochemical pathways NOT indicated by the genome annotation and known biochemistry of *Y. pestis*. For example, the utilization of several carbon sources was not previously reported in the literature, are not indicated in the genome annotations (Ann's refs), and are not in the enzyme database. Further, we found that the utilization of these chemicals is dependent on the bacterial strain and whether the bacteria were grown under conditions mimicking the mammalian host or the flea vector. Significant differences were also detected between virulent inducing and vector growth conditions, and between same species strains with diverse virulence levels.

Preliminary experiments also link virulence factor expression to the differences in metabolic pathways. Additional work has previously linked virulence factor expression with quorum sensing (in preparation). Taken together, there are implications for whether biomarker detection could contain false negatives depending on the growth substrate(s) of the bacteria. Combining phenotypic characterization with pathway information, proteomic profiling and host response of diverse pathogen isolates provides a novel approach to threat characterization via a holistic or Systems Biology view.

Virulence Characterization. We have developed a real-time reporter system to monitor the thermal induction of virulence factors in *Y. pestis* based on introduction of a reporter plasmid in *Y. pestis* in which the expression of enhanced green fluorescent protein (EGFP) is under the control of the promoters for virulence factors. Induction of the expression of these genes *in vivo* is determined by the increase in fluorescence intensity of EGFP in real time, in 96-well format. Several virulence factors were determined to be differentially expressed in response to the temperature shift associated with the change from the physiological environment of the flea to that of the mammalian host, i.e. 26°C to 37°C [26]. This system has provided a unique method to rapidly determine the effects of host, pathogen and environmental stimuli on virulence factor induction in *Y. pestis* in real time, in living cells.Specifically, we determined that quorum sensing and a host factor increase virulence factor expression.

Due to variability in the real-time assay early following temperature shift, the effect of spent media on the thermal induction of virulence factor genes in *Y. pestis* was tested with the hypothesis that quorum sensing may have caused the variability. The rate of increase of the thermal induction of virulence factor genes was greater when the experiment is performed in partially spent media than when performed in fresh media (**Figure 4A**), raising the possibility that quorum sensing molecules may be present in spent media and might further play a role in the expression of virulence factors in *Y. pestis*. Therefore, the presence of acylhomoserine lactone (AHL) quorum sensing signaling molecules in spent media was analyzed using LC-MS/MS. Spent media was extracted with methylene chloride, and the dried samples reconstituted in aqueous formic acid and analyzed by mass spectrometry. Four AHLs were detected in the spent media and identified as N-3-oxo-hexanoylhomoserine lactone, N-3-oxo-octanoylhomoserine lactone, N-hexanoylhomoserine lactone (C6-HSL) and N-octanoylhomoserine lactone (C8-HSL). The addition of commercially available, purified C6-HSL and C8-HSL to *Y. pestis* media also increased the rate of virulence induction over fresh media alone, similar to effect of spent media.

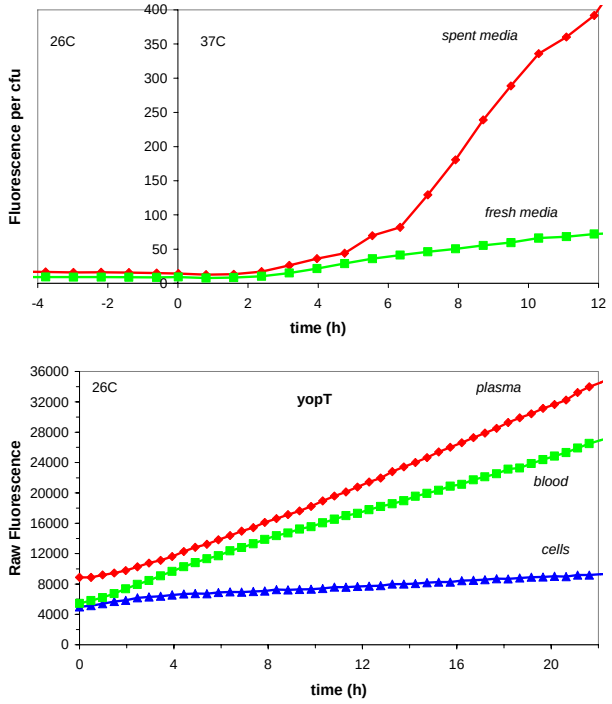

Fig. 4. Effect of human whole blood, plasma, and blood cells on yopT induction. A) The use of spent media resulted in increased virulence factor production. **B)** Human plasma resulted in increased virulence factor expression without the thermal shift.

The effect of human blood on the thermal induction of virulence factor genes in *Y. pestis* was also tested. Surprisingly, the induction of reporter genes was observed with addition of a 1:11 dilution of whole blood to strains grown at 26°C, unlike the studies discussed above where the induction is only observed after the temperature is shifted from 26°C to 37°C. In order to determine the component of whole blood responsible for the induction at 26°C, blood was fractionated into plasma and cellular components by centrifugation. The effect of the addition of a 1:11 dilution of either whole blood, plasma, or blood cells was assayed in our EGFP-reporter assay (**Figure 4B**). This experiment demonstrated that plasma, rather than the cellular fraction of whole blood, stimulated virulence factor induction at 26°C. This effect is independent of the addition of 4mM $CaCl_2$ to the media. Though the composition of human plasma is extremely complex, one of the most abundant classes of plasma proteins are immunoglobulin molecules and via a series of experiments, we determined that IgG stimulates virulence induction at 26°C in the EGFP-reporter assay.

The importance of these findings are relevant to mechanistic understanding of Y. pestis; however, the finding that Y. pestis virulence may be induced by antibody binding has direct implications to detection efforts that utilize antibodies for pathogen identification. Further, this real-time approach affords a novel means to characterize pathogens where the mechanism of virulence is unknown, such as Francisella tularensis, to rapidly identify functional signatures.

<u>*Host Response.*</u> To address the ability to distinguish between exposure to more closely related pathogens for surveillance of infectious diseases, host response to three human pathogens from the *Yersinia* family was characterized by 2-DE and mass spectrometry, following *in vitro* exposure of human macrophage cells to *Y. pestis*, *Y. pseudotuberculosis* and *Y. enterocolitica* [22]. As an example of distinct host response, peroxiredoxin III, a known part of the mitochondrial antioxidant system, was upregulated following exposure to *Y. pestis*, but not after exposure to the near neighbor pathogens. Oxidative stress in the host mitochondria may reflect the virulent nature of *Y. pestis*. While this report was able

to distinguish between pathogen exposures, a noted limitation was the use of traditional 2-DE, which suffers from low sensitivity and gel-to-gel variation. The issue of sensitivity, however, surprisingly did not affect the ability to detect several *Yersinia* virulence factors in the cytosolic fraction of host cells after pathogen exposure. It is unclear if this is due to an experimental artifact of the 5:1 pathogen to host cell ratio, or if pathogen proteins can realistically be detected inside host cells. We are further investigating this using advanced proteomic technologies.

Subsequent to this initial report, a complementary study with improved sensitivity through use of multiplexed fluorescent dyes and reduced experimental variability via inclusion of an internal standard on all gels was used [20]. Subcellular proteomic fractions of human monocytes exposed to *Y. pestis* and *Y. pseudotuberculosis* were characterized. Specifically, proteins from cytoplasmic, nuclear and membrane fractions of monocytes cells were examined by 2-D DIGE and mass spectrometry. A total of 16 differentially expressed host proteins were identified after *Y. pestis exposure*, and 13 host proteins were identified after *Y. pseudotuberculosis* exposure. Only two of these differentially expressed proteins identified were shared between the two exposures. The proteins identified in this study are reported to be involved in a wide spectrum of cellular functions and host defense mechanisms including apoptosis, cell signaling, cytoskeletal rearrangement, DNA replication and transcription, metabolism, protein folding, and protein synthesis and degradation.

Two proteins identified in this study of particular interest are valosin containing protein p97, which was significantly upregulated by *Y. pestis* but not by *Y. pseudotuberculosis* exposure; and heat shock protein 90 or HSP90, which was downregulated by *Y. pseudotuberculosis* but not by *Y. pestis* exposure [20]. P97 is a molecular chaperone that targets many ubiquitinated substrates to the proteasome for degradation including cytokine receptors of IL-9 and IL-2. This result is suggestive of *Y. pestis* evasion of host immune response via targeted degradation of cytokines or, more generally, that *Y. pestis* causes increased degradation of ubiquitinated proteins for the purpose of antigen presentation. Interestingly, HSP90 is a molecular chaperone, reported to interact with several proteins including survivin. It was previously demonstrated that the disruption of the survivin-HSP90 complex results in proteasomal degradation of survivin and subsequent cellular apoptosis [77]. Thus, the down-regulation of HSP90 indicates increased apoptosis following *Y. pseudotuberculosis* exposure. Results from this study indicate that exposure to even closely related pathogens can be distinguished based solely on host response. This study has guided *ex vivo* and *in vivo* studies also discussed here, and also has significant implications for early detection of infectious diseases.

Multiple strains of *Y. pestis* and *B. anthracis* as well as multiple near neighbors have also been exposed to whole blood *ex vivo*. In order to identify differences in host response, cytokine levels were measured using a human cytokine protein array (Zyomyx, Hayward, CA) in a multiplexed quantitative assay. Distinct cytokine profiles were detected that clearly discriminated between seven different pathogen exposures as shown in a heat map representation of the data (**Figure 5**). Notably, host response could distinguish the following pathogen exposures: virulent from avirulent pathogens; *Y. pestis* from *B. anthracis*; near neighbors from each other; and, most strikingly, two virulent clinical isolates of *Y. pestis* that exhibit 1000-fold difference in virulence levels in a rodent model. While these results are interesting and potentially revealing with regard to virulence mechanisms, we are extending their studies to compare *ex vivo* to *in vivo* rodent response in order to determine the efficacy and applicability of using whole blood to dissect disease pathways and define biomarkers for detection of infectious disease. Of additional note, traditional immunological assays were used to confirm several of the cytokine expression levels.

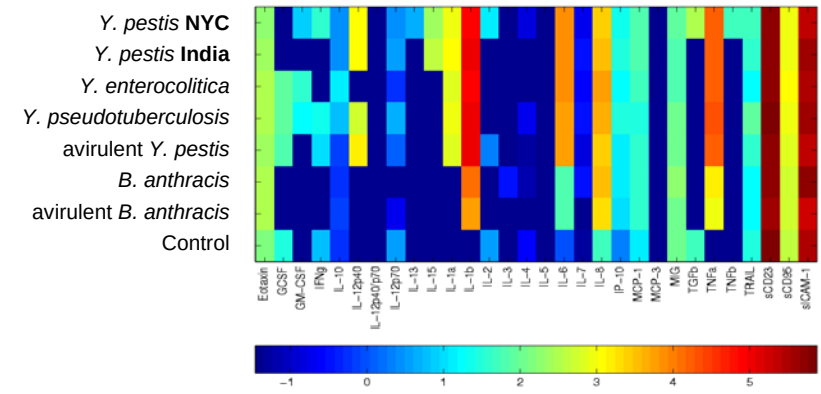

Fig. 5. Heat map of cytokine expression levels in human whole blood model following exposure to 7 pathogens.

While *in vitro* and *ex vivo* studies are of practical importance in the study of host-pathogen interactions, *in vivo* host response to infection reflects multiple cell types, tissues, and interactions, in addition to signaling events and cascades of expression. Thus, to fully understand host-pathogen interactions, *in vivo* models are crucial. It is, however, extremely valuable to leverage and compare results from *in vitro, ex vivo* and *in vivo* studies to determine when a simpler model will suffice versus when an animal model is more relevant. It should also be noted, however, that while animal models can be utilized as a means to project human response to an infectious disease, the most appropriate model systems need possess similar pathogen lifecycle and disease pathway in order to be directly applicable to characterization of human disease.

The murine model of plague has been widely used to study pathogenesis and host-pathogen interactions, but has been insufficiently characterized in terms of clinical, immunological, and pathological effects of infection. The objective of our work was to perform *in vivo* intra-peritoneal infection mice with several strains of *Y. pestis,* comparing dose needed to induce mortality, clinical effects, pathology, and some immune parameters including complete blood counts, cytokine responses in blood and tissue, bacteriological dynamics by culture and polymerase chain reaction (PCR). Much of our ongoing *in vivo* work has emphasized clinicopathologic sequelae of infection with *Y. pestis* NYC, CO92, and India-195 in a mouse model. An ED_{50} (effective dose approximating LD_{50}) was determined for each strain using the "up and down method". In the present study, greater doses of *Y. pestis* India-195 were required to induce disease than *Y. pestis* NYC, confirming that the former strain was considerably less virulent than *Y. pestis* NYC. Unfortunately, the entire isolation and passage history of *Y. pestis* India-195 could not be recovered, but it was purported to have originated from a bubonic human case in India-195 and to have been passed numerous times in the laboratory, which may have contributed to its becoming attenuated (von Metz et al., 1971)(K. Smith, LLNL, pers. comm.). rom an ancestral *Y. pseudotuberculosis* clone 1500-20,000 years ago (Achtman et al., 1999).

Major differences in ED_{50} were detected among the bacteria, with 50% of mice dying in approximately 3-5 days after receiving $5x10PP^4$ colony forming units (cfus) intraperitoneally of NYC, 1×10^4 cfus of CO92, 1×10^7 cfus of India-195. Most rodents showed little prodromal evidence of infection before they became moribund: clinical signs included inappetence, non-responsiveness to gentle tactile stimuli, and dehydration assessed by skin turgor, mucous membrane tackiness, and sunken ocular globe.

Mice infected with *Y. pestis* NYC had leukopenia (2,239 leukocytes/µl; 123 s.d.) but not anemia; platelet counts were reduced (mean 123,176/µl; 33,361 s.d.). One mouse (P51) with *Y. pestis* NYC infection had numerous extracellular *Y. pestis* organisms in the blood smear. Mice with terminal *Y. pestis* infection tended to have degenerative left shifted hemograms with evidence of neutrophilic toxicity and some intracellular bacteria. Statistical assessment confirmed that there were significant differences among groups in leukocyte counts ($P = 0.004$), platelet counts ($P = 0.005$), and hematocrit ($P = 1.2 \times 10^{-5}$).

Culture was performed on blood and tissue samples. Spleen, liver, lung and blood often were positive on day 3 PI of all three treatment groups. Spleen and liver tended to be culture-positive most commonly, with lung and blood less commonly culture-positive. Ninety-100% of spleens and livers from mice with *Y. pestis* NYC were positive, while approximately 80% of lungs and 75% of blood samples were. Mice with *Y. pestis* India were considerably less likely to be culture positive, with no recovery of bacteria from blood, and positive culture in only 10% of lungs, 35% of livers, and 50% of spleens, despite the mice appearing clinically moribund. Differences in culture recovery among the three strains and among organs were statistically significant ($P = 0.007$). A real-time PCR assay was applied to amplify fragments of the *pla* and *asn*-tRNA genes. As expected, all control mice and mice infected with *Y. pseudotuberculosis* were PCR-negative in all tissues tested. Mice infected with *Y. pestis* India were consistently *asn*-tRNA negative in all tissues, consistent with earlier sensitivity analysis of this PCR protocol for asn in India-195. PCR for the pla gene validated the bacterial culture and documented comparable amounts of bacterial DNA between *Y. pestis* India-195 and NYC-infected mice. The lowest C_T (indicating greatest amount of DNA) was found in both treatments in spleen, with highest C_T values in blood for India and lung for NYC.

Cytokine profiles were performed to evaluate possible changes in IL-10, TNF-α, IFN-γ, IL-1β, using GAPDH as a calibrator. No significant differences in cytokine transcription were detected in blood, liver, or spleen, among the three *Yersinia* spp. challenges and a negative control. However, lung tissue showed statistically significantly increased transcription in all four cytokines tested. For IFN-γ, lung tissue infected with *Y. pestis* NYC had 180-fold increased transcription compared to *Y. pestis* India and the negative control (all of which were comparable) ($P = 7.89 \times 10^{-17}$). IL-10 was 78 times upregulated in *Y. pestis* NYC, compared with *Y. pestis* India ($P = 0.007$), IL-1β was 805 times upregulated in *Y. pestis* NYC compared with *Y. pestis* India ($P = 3.29 \times 10^{-12}$), and TNF-α was 3304 times upregulated ($P = 1.06 \times 10^{-13}$).

Spleen, lung and liver from 6 mice with *Y. pestis* India and 6 with *Y. pestis* NYC were examined. Consistent lesions were observed in the lung, ranging from mild to severe and were characterized by acute neutrophilic interstitial pneumonia with regional collapse of alveoli and protein-rich exudate filling alveolar spaces (**Figure 6**). Focal necrosis of alveolar septae was identified in the most severe cases. Many sections also exhibited mild to moderate vascular changes. Affected small arterioles and veins featured numerous plump endothelial cells, often with crenated or pyknotic nuclei, which often appeared lifted from the underlying basement membrane (interpreted as vascular reactivity). In the most severely affected animal, there was separation of smooth muscle fibers and hylanization of the tunica media with rare migrating inflammatory cells (mild vasculitis). Splenic samples also regularly exhibited pathologic changes consistent with an acute inflammation and necrosis. Changes were considered severe in 7/12 mice and mild to moderate in 5/12 mice. The severely affected spleens exhibited acute, multifocal to coalescing necrosuppurative splenitis characterized by degenerate and nondegenerate neutrophils and admixed with fibrin and pyknotic cellular debris. These well demarcated necrosuppurative foci were regularly located at, and appeared to be arising from, the marginal zone between the white and red pulp. Small numbers of intralesional Gram-negative bacilli were identified within the spleen of 3 mice. In one severely affected spleen, the lesion consisted of diffuse necrosis, with sparse neutrophilic inflammation, of red pulp with massive numbers of intralesional Gram-negative bacilli. Liver samples were inconsistently (5/12 animals) affected by a multifocal or regionally extensive, acute hepatocellular necrosis. In the affected animals the liver sample typically had 1-2, small or focally extensive areas of acute coagulative necrosis of hepatocytes without inflammation. The most severely affected liver exhibited numerous clusters of gram negative, rod-shaped bacteria within sinusoids, in addition to multifocal acute hepatocellular necrosis.

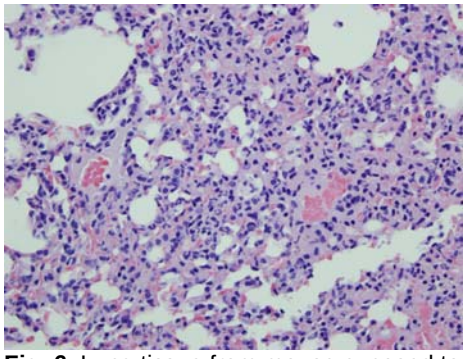

Fig. 6. Lung tissue from mouse exposed to *Y. pestis* NYC showing acute neutrophilic interstitial pneumonia with vascular reactivity suggestive of pneumonic plague.

Overall, the failure to document bacteria in all affected tissues and the histopathological appearance of the tissues suggested that the actual cause of death was severe inflammatory response syndrome (SIRS) and endotoxic shock, accompanied by severe pneumonia and hypoxemia in several mice. We have additional preliminary information on plague infection in deer mice, *Peromyscus maniculatus*, as well. We performed both intradermal and IP inoculation using the NYC strain in 2 *P. maniculatus* individuals. Morbidity was not observed and all individuals survived the original 4 day period during which laboratory mice had developed fatal plague. However, although delayed, death was induced in the deer mice on average 10 days post-inoculation, both in ID and IP routes of inoculation. Bacterial culture confirmed presence of *Y. pestis* terminally in blood, spleen, liver, and lungs of all individuals. Further characterization of host responses and bacterial virulence factors will help with an understanding of mechanisms of plague morbidity and mortality as well as ultimately early diagnostic and interventive strategies for plague.

The pathogenesis of disease in human plague is not fully understood, although insights from the mouse model could be informative for appreciating bacterial-host interactions in human disease. Lesions in the spleen, liver, and lung of people with plague often are hemorrhagic and necrotic, but tend to have few neutrophils, evidence of the anti-inflammatory effects of Yops and other *Y. pestis* virulence factors. Necrosis in humans, as in mice, is prominent (Smith and Reisner, 1997). The peripheral leukogram reflects a spectrum from leukopenia to leukocytosis with a leukemoid reaction. Many

untreated cases of bubonic plague, as well as pneumonic plague cases, develop severe interstitial, followed by hemorrhagic, necrotizing bronchopneumonia. The alveoli contain bacteria and proteinaceous effusion with necrotic and hemorrhagic alveolar septae. In humans, there also is evidence of a cardiotoxin and pulmonary edema. The pathogenesis of pneumonia in septicemic plague is not understood. Most cases of pneumonic plague are induced by inhalational exposure to the bacterium, although some cases arise for unknown reasons as complications of bubonic plague. Thus it was particularly interesting that such fulminant pneumonia and cytokine dysregulation occurred in mice in the present study even after IP inoculation of the bacterium, suggesting some degree of tropism of the bacteria for the lungs.

Other *in vivo* host-pathogen interaction studies using higher animal models including bovine Brucella in collaboration with the Texas A&M University DHS Center of Excellence (Dr. G. Adams) and swine SEB in collaboration with Walter Reed Army Institute of Research (Dr. M. Jett) will be characterized next in order to expand our "Host Response Library".

Conclusions and Future Directions

Knowledge gained from host-pathogen interactions, as described within, can provide pathogen-specific signatures for rapid pathogen detection and characterization of pathogen release and infectious diseases. The ultimate goal of early and specific detection is to increase the window of opportunity for response and treatment in the event of an outbreak or intentional BT event. We proposed that establishment of a "Host Response Library" and a "Pathogen Reference Library" will be extremely useful in presymptomatic and presyndromic sentinel monitoring or surveillance of infectious diseases and in characterizing emergent, unusual or engineered pathogens for threat assessment. There also exists a dual benefit, in addition to surveillance and threat characterization, in the ability to screen large numbers of individuals who may have been exposed following a pathogen release. Thus, by identifying signatures to protect against the rare event of bioterror, our approach will also enhance human health through the ability to rapidly respond to an epidemic of intentional, accidental or natural causes. From a detection perspective, our ultimate vision is that of a dipstick, mouthswab, or breathalyzer type diagnostic for infectious diseases and presence of a pathogen, based on information garnered from host-pathogen interaction studies.

Acknowledgments. This work was funded by the Department of Homeland Security (Biological Countermeasures Program). This work was performed under the auspices of the U.S. Department of Energy by University of California Lawrence Livermore National Laboratory under contract No. W-7405-Eng-48.